

Aqueous Immiscible Layered Double Hydroxides: Synthesis, Characterisation and Molecular Dynamics Simulation

Kanittika Ruengkajorn,^{a,†} Valentina Erastova,^{*,b, †} Jean-Charles Buffet,^a H.
Chris Greenwell^{*,c} and Dermot O'Hare^{*,a}

^aChemistry Research Laboratory, University of Oxford, 12 Mansfield Road, OX1 3TA, UK

^bDepartment of Chemistry, Durham University, Lower Mountjoy, South Road, Durham, DH1 3LE

^cDepartment of Earth Sciences, Durham University, Science Labs, Durham, DH1 3LE

Table of contents

1. General experimental details	S2
1.1. Analytical techniques for LDH characterisation	S2
1.2. Synthesis of Conventional, AMO- and AIM-LDHs	S3
2. General molecular simulation details	S4
2.1. LDH model	S4
2.2. Solvents	S4
2.3. Force field parameters	S4
2.4. Simulations	S4
2.5. Visualisation	S4
2.6. Analysis	S5
3. Supplementary experimental data	S6
4. Supplementary molecular simulation data	S12
5. References	S16

1. General experimental details

1.1 Analytical techniques for LDH characterisation

1.1.1. X-ray powder diffraction (XRD)

X-ray powder diffraction (XRD) results were investigated by using a PANalytical X'Pert Pro diffractometer in reflection mode operating at a voltage of 40 kV and a current intensity of 40 mA with Cu-K α radiation ($\lambda = 1.5406 \text{ \AA}$). LDHs and LDOs powder were placed into stainless steel sample holders.

A 1° slit was used. Bragg reflections due to sample holder were observed at $2\theta = 43\text{-}44^\circ$ and 50° and from silicon wafer were located at $2\theta = 33^\circ, 62^\circ$ and 69° .

The Scherrer's equation was used to estimate the mean crystallite domain length (CDL) of the LDHs; $CDL = K\lambda(\beta\cos\theta)^{-1}$, where CDL = the mean crystallite domain length, K = Scherrer constant, λ = the wavelength of the radiation, and β = the full-width at half-maximum height (FWHM) values of a reflection located at 2θ . Thus, the CDL along *c*-axis (CDL₀₀₃) can be calculated from the full-width at half-maximum height values of the (003) Bragg reflection, which is assumed to be the total crystal thickness along the *c*-axis. Moreover, a layer thickness of LDHs from the d_{003} spacing using the Bragg's law; $n\lambda = 2d(\sin\theta)$, *n* is assumed to be one. Therefore, by application of the Bragg's law and the Scherrer equation, the number of LDH layers can be estimated.

1.1.2. Fourier transform infrared spectroscopy (FTIR)

Fourier transform infrared (FTIR) spectra of samples were recorded on Thermo Scientific Nicolet iS5 FTIR spectrometer in attenuated total reflectance (ATR) mode. Spectra were obtained in the range of 600-4000 cm^{-1} ; 50 scans with 4 cm^{-1} resolution.

1.1.3. Transmission electron microscopy (TEM)

Transmission electron microscopy (TEM) was conducted at the Research Complex at Harwell on Jeol JEM-2100 TEM equipped with LaB6 filament at an accelerating voltage of 200 kV. Prior to analysis, samples were diluted with deionised water and sonicated in deionised water for 15 minutes. A few droplets of the resulting suspension were left to dry on a copper grid covered with a carbon film (300 mesh, Agar scientific).

1.1.4 Thermogravimetric analysis

Thermogravimetric analyses were performed by using a Mettler Toledo TGA/DSC 1 system. 15 mg of sample (LDHs) was loaded into alumina crucible and heated from 30–800 $^\circ\text{C}$ at a rate of 5 $^\circ\text{C}/\text{min}$ under a flow of dry N_2 . Differential thermogravimetric analysis (DTG) is obtained from the 1st derivative of TGA data.

1.1.5. Elemental analysis (EA)

Elemental C, H, N analysis was performed by a quantitative oxidative combustion technique by Mr Stephen Boyer at London Metropolitan University.

1.1.6. Density

Tap densities were determined by standard testing method (ASTM D7481-09) using a graduated cylinder. The powder was filled into a volumetric cylinder and a precise weight of sample (m) was measured. The volume was measured before (V_0) and after 1000 taps (V_t). The loose bulk and tap densities were calculated by: Loose bulk density = m/V_0 ; Tap density = m/V_t .

1.2. Synthesis of Conventional, AMO and AIM LDHs

1.2.1 Synthesis of flower shape like Mg_4Al-CO_3 LDHs *via* co-precipitation method

Mg_4Al-CO_3 LDHs flower like shape were synthesised and treated with solvent using a method adapted from Wang *et al.* and Chen *et al.*.

The mixed metal salts solution of $Mg(NO_3)_2 \cdot 6H_2O$ (80 mmol) and $Al(NO_3)_3 \cdot 9H_2O$ (20 mmol) in 50 mL deionised water was added dropwise into 50 mL of 25 mmol Na_2CO_3 solution while stirring for 1 hour. Constant pH of 10 was maintained by addition of 4 M NaOH to the reaction mixture using an auto-titrator (Syrris, Atlas Syringe Pump) at feeding rate of 5 mL/min. After stirring at room temperature for 24 hours, the product was filtered and washed with deionised water until pH 7. Then the wet cake was re-dispersed in 100 mL of deionised water and divided into four portions. Each portion was filtered and rinsed with 500 mL of a washing solvent then re-dispersed and stirred in 300 mL of this solvent at room temperature for 4 hours. The solvent was removed by filtration and the obtained LDH was further rinsed with 200 mL of this solvent. The product was dried at room temperature in vacuum. Mg/Al ratio of 4 is assumed.

Mg_2Al-CO_3 LDH and Mg_3Al-CO_3 LDH were prepared using similar procedure as mentioned above. The mixed metal solution was prepared using 50 mL aqueous solution of 33.3 and 37.5 mmol of $Mg(NO_3)_2 \cdot 6H_2O$ and 16.7 and 12.5 mmol of $Al(NO_3)_3 \cdot 9H_2O$, for Mg_2Al-CO_3 LDH and Mg_3Al-CO_3 LDH, respectively. Then the same procedure as mentioned above was used.

1.2.2. Effect of solvent types: AMO vs. AIM solvents

Both AMO and AIM solvents were compared in this study. The AMO solvent was ethanol, the AIM solvents were ethyl acetate, diethyl ether, hexane and toluene.

2. General molecular simulation details

2.1 LDH model

For molecular dynamics simulation an atomistic model of LDH is built. Here we use a unit of LDH with the stoichiometry $[\text{Mg}_3\text{Al}(\text{OH})_8]^+$, with one positive charge per unit cell, counterbalanced by 0.5 carbonate ions. In order to simulate a reasonably large model system and to avoid self-interaction artefacts, the unit cell was replicated in a 5 x 6 array, creating a 3.82 nm by 2.75 nm LDH surface. The LDH layer thickness is 0.53 nm and the layer occupies the region between $z = 0$ and 0.55 nm. A simulation box was obtained by adding 4 nm of vacuum above the surface.

2.2. Solvents

The vacuum described above was filled with different solvents to create solvated LDH surfaces. A system containing pure water (WAT) was simulated. Three different systems containing 1400, 1000 and 800 water molecules were run. Water-solvent mixtures to model step wise washing with solvent were also set up as follows: 100 solvent to 1000 water molecules (1 : 10 ratio); 200 solvent to 600 water molecules (1 : 3 ratio) and 300 solvent to 300 water molecules (1 : 1 ratio). The solvent was varied between ethanol (ETH), ethyl acetate (EA), diethyl ether (DE), hexane (HEX) and toluene (TOL).

2.3. Force field parameters

The ClayFF force field¹ was used to model the LDH within the simulations. This force field is specifically developed to model clay-like minerals, including LDHs. The charges were adjusted to create a net positive +1 per unit cell, as described in an earlier paper by the authors.² The CHARMM36 force field^{3,4} was used to model the organic solvents and the force field parameters were assigned via the CGenFF algorithm.⁵ ClayFF has been tested previously and used by the present authors with the CHARMM force field.^{6,7} Both force fields are parameterized for use with SPC water, used in this work.

2.4. Simulations

The simulations were performed with GROMACS 4.6.7.^{8,9} Periodic boundary conditions coupled with a large supercell were used to avoid finite size effects. Each simulation was first energy minimized using a steepest descent algorithm with convergence criterion being the maximum force on any one atom to be less than $100 \text{ kJ mol}^{-1} \text{ nm}^{-1}$. The system was then equilibrated for 0.5 ns in the isothermal–isobaric (NPT) ensemble with a velocity-rescale Berendsen thermostat set at 300 K and the temperature coupling constant set to 0.1 ps. A semi-isotropic Berendsen barostat was used, set at 1 bar, with a pressure-coupling constant of 1 ps. The minimization and equilibration simulations were run with real-space particle-mesh-Ewald (PME) electrostatics and a van der Waals cutoff of 1.2 nm. After equilibration, a production run of 20 ns was performed. This was run with PME electrostatics and a van der Waals cutoff of 1.4 nm in NPT ensemble, with the same parameters as in the equilibration.

2.5 Visualisation

The snapshots were produced with VMD 1.9.2¹⁰ and the atoms were rendered with the following color scheme: Mg atoms pink, Al cyan, O red, H white, C gray, S in yellow and Cl

blue. Due to system periodicity, the same LDH layer visually appears on both sides of the box.

2.6. Analysis

The density, basal interlayer d-spacing and partial density analysis were performed with GROMACS tools. H-bond analysis was developed and performed with a VMD TCL script, where an H-bond was defined to be at a maximum distance of 3.5 Å between the hydrogen donor and acceptor, and at a maximum angle of 30° between the donor–hydrogen–acceptor. H-bonds were counted using a 1 Å sliding window moving along the z-axis with 0.25 Å steps. The vectorial analysis was developed in-house. A vector between two atoms is assigned and defined for each species as follows (Figure S16): ethanol - between the alpha-carbon and oxygen; ethyl acetate - from ether oxygen to carbonyl oxygen; diethyl ether - centre between carbons and oxygen; hexane - between carbons of methane groups; toluene - between centre of benzene ring and methane group. For every solvent molecule, the elevation of its vector with respect of the LDH surface was calculated. Elevations were then collected using a sliding window, as for the H-bond analysis. All data analysis was carried out over the last 10 ns of simulation. The partial density, H-bond density and vectorial analysis were plotted only up to 1.8 nm from the surface for clarity, as the solvent properties were no longer influenced by the surface beyond 1.5 nm distance. All data was plotted with Matplotlib.¹¹

3. Supplementary experimental data

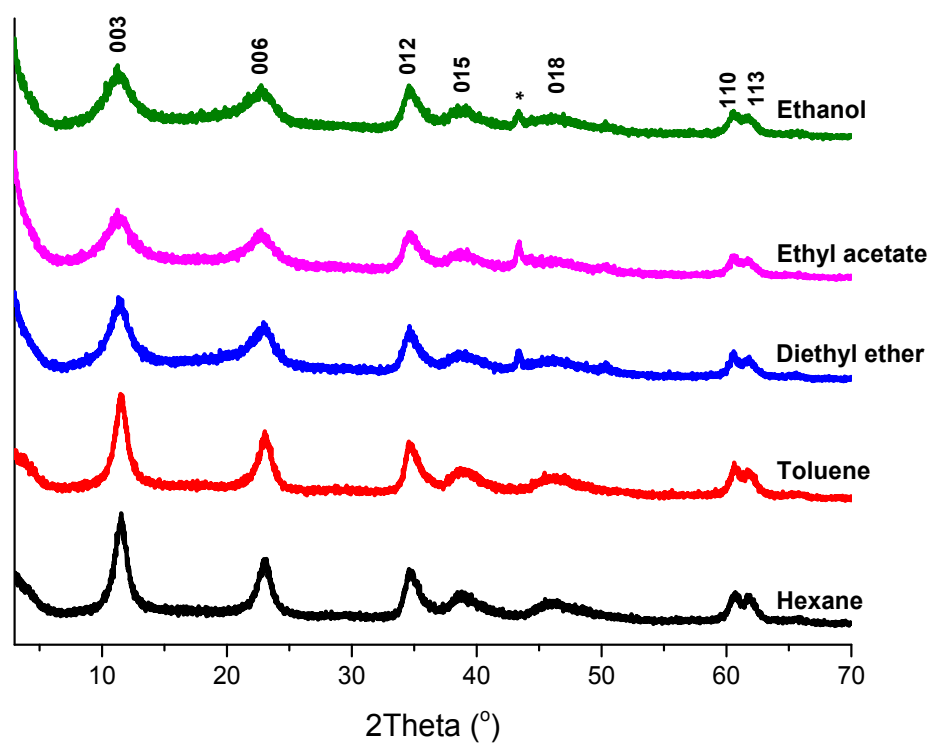


Fig. S1 Powder X-ray diffraction patterns of different solvent-treated Mg_4AlCO_3 -LDHs. * is a Bragg reflection from the Al sample holder.

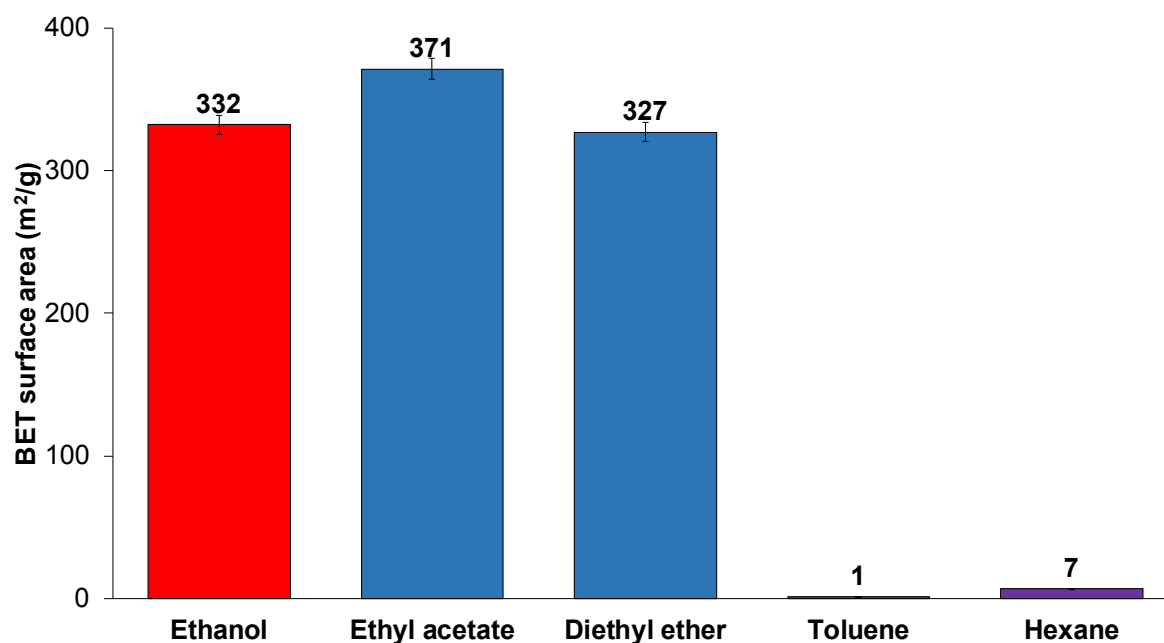


Fig. S2 BET surface area of different solvent-treated Mg_4AlCO_3 -LDHs.

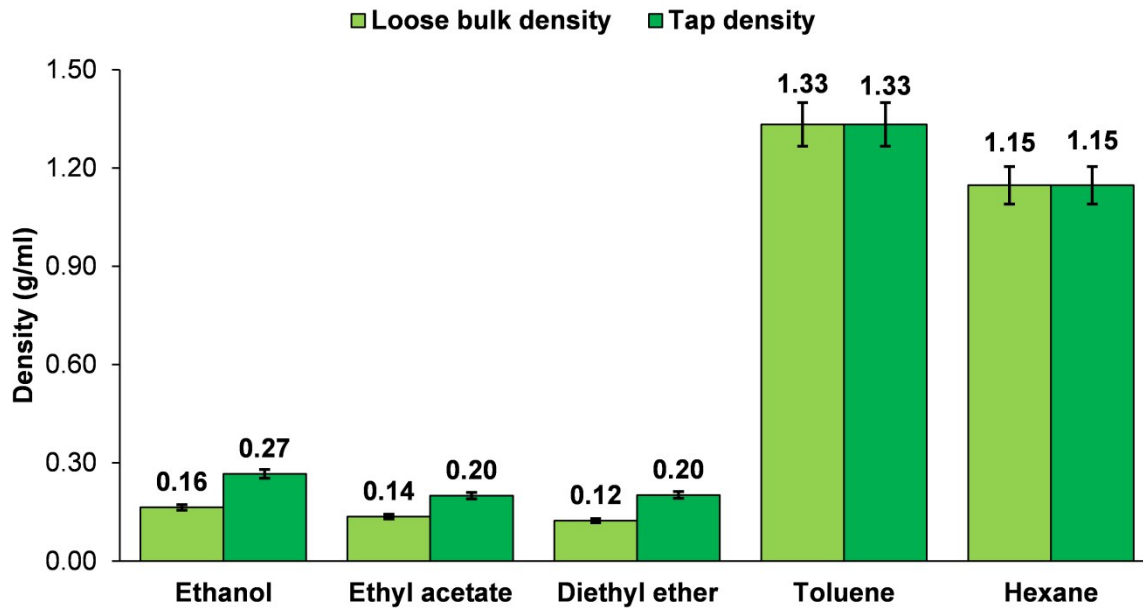


Fig. S3 Loose bulk and tap densities of different solvent-treated LDHs.

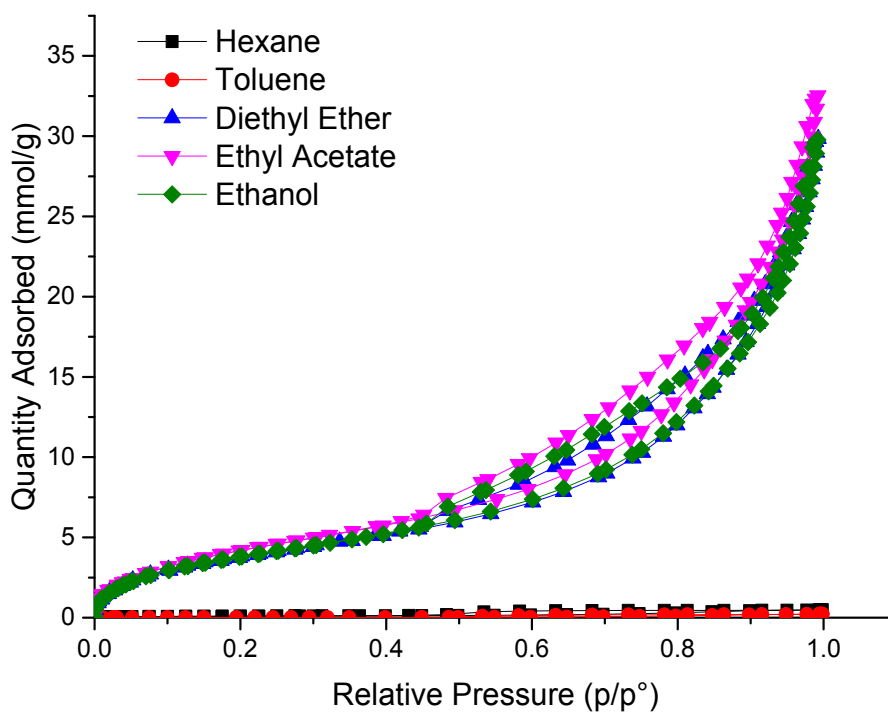


Fig. S4 BET isotherm of different solvent-treated Mg_4Al-CO_3 LDHs.

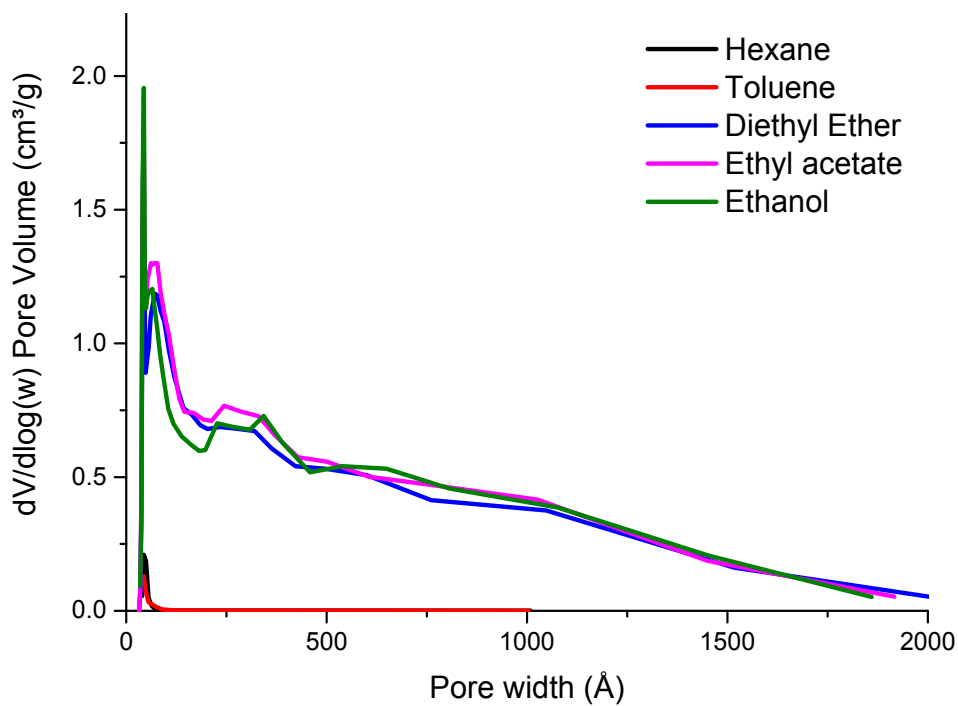


Fig. S5 Pore size distribution of different solvent-treated Mg_4Al-CO_3 LDHs.

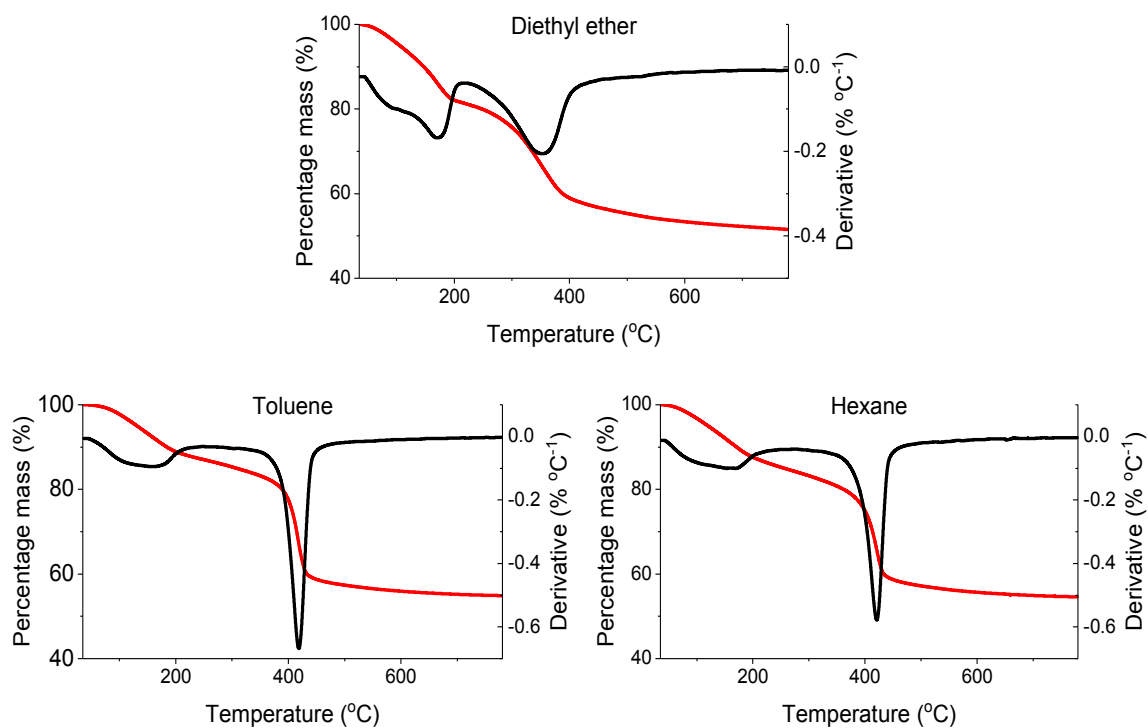


Fig. S6 TGA and DTG curves for AIM-LDHs.

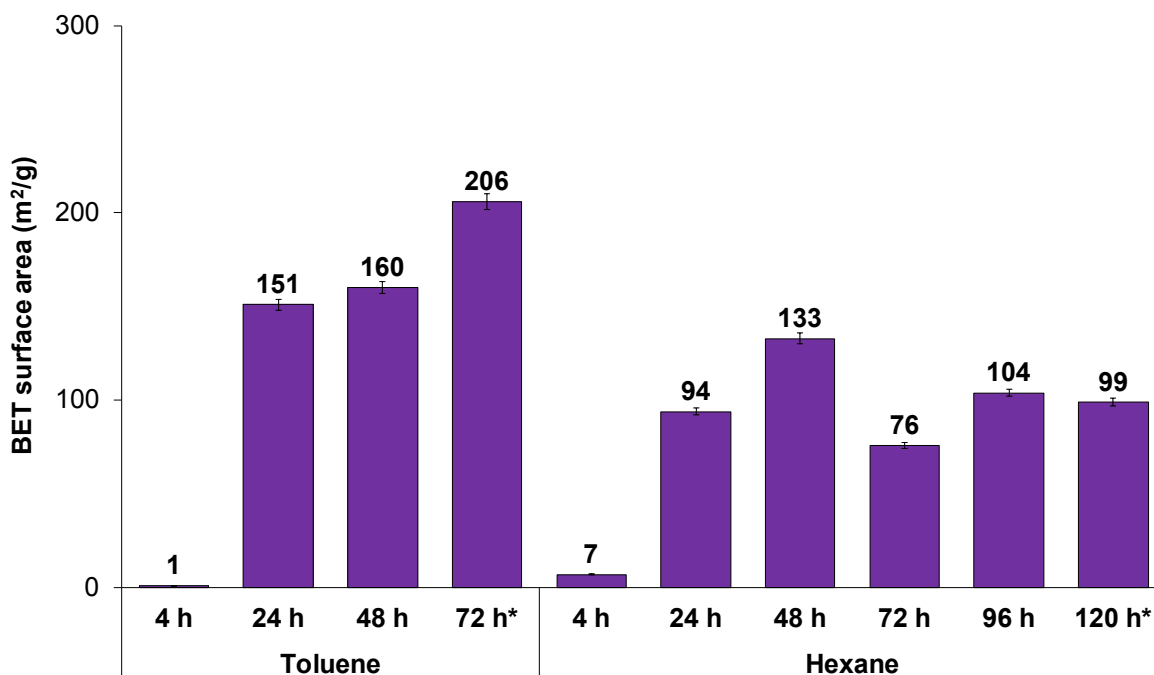


Fig. S7 BET surface area of Mg₄Al-CO₃-LDH washed different weak H-bond solvents with varies dispersion time. * is time to reach full dispersion.

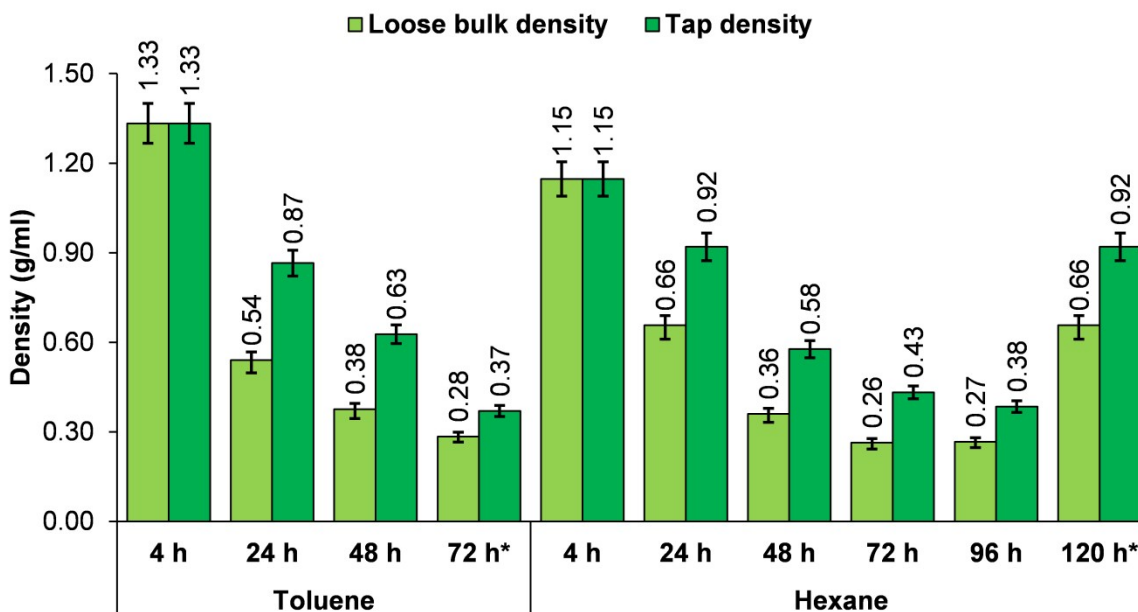


Fig. S8 Loose bulk and tap densities of Mg₄Al-CO₃-LDH washed different weak H-bond solvents with varies dispersion time. * is time to reach full dispersion.

Table S1a. Summary of water (b) and solvent content (c) in the AMO-LDHs and AIM-LDHs as determined by elemental analysis

Washing solvent		b	c	Formula of LDHs	%C			%H		
					#1	#2	Average	#1	#2	Average
AMO solvents	Ethanol	0.245	0.215	$[\text{Mg}_{0.80}\text{Al}_{0.20}(\text{OH})_2(\text{CO}_3)_{0.10}] \cdot 0.245\text{H}_2\text{O} \cdot 0.215(\text{Ethanol})$	8.93	8.99	8.96	4.79	4.78	4.79
AIM solvents	Ethyl acetate	0.319	0.065	$[\text{Mg}_{0.80}\text{Al}_{0.20}(\text{OH})_2(\text{CO}_3)_{0.10}] \cdot 0.319\text{H}_2\text{O} \cdot 0.065(\text{Ethyl acetate})$	6.52	6.59	6.56	4.14	4.17	4.16
	Diethyl ether	0.370	0.021	$[\text{Mg}_{0.80}\text{Al}_{0.20}(\text{OH})_2(\text{CO}_3)_{0.10}] \cdot 0.370\text{H}_2\text{O} \cdot 0.021(\text{Diethyl ether})$	3.76	3.83	3.80	4.01	4.09	4.05
	Toluene	0.402	0.001	$[\text{Mg}_{0.80}\text{Al}_{0.20}(\text{OH})_2(\text{CO}_3)_{0.10}] \cdot 0.402\text{H}_2\text{O} \cdot 0.001(\text{Toluene})$	2.51	2.57	2.54	3.87	3.95	3.91
	Hexane	0.548	0.002	$[\text{Mg}_{0.80}\text{Al}_{0.20}(\text{OH})_2(\text{CO}_3)_{0.10}] \cdot 0.548\text{H}_2\text{O} \cdot 0.002(\text{Hexane})$	2.66	2.63	2.65	4.19	4.19	4.19

Table S2. Summary of water and solvent content in the AIM-LDHs from different weak H-bond solvents with varies dispersion time determined by elemental analysis

Weak H-bond solvents	Dispersion time	b	c	Formula of LDHs	%C			%H		
					#1	#2	Average	#1	#2	Average
Toluene	4 h	0.402	0.001	$[\text{Mg}_{0.80}\text{Al}_{0.20}(\text{OH})_2(\text{CO}_3)_{0.10}] \cdot 0.402\text{H}_2\text{O} \cdot 0.001(\text{Toluene})$	2.51	2.57	2.54	3.87	3.95	3.91
	24 h	0.532	0.004	$[\text{Mg}_{0.80}\text{Al}_{0.20}(\text{OH})_2(\text{CO}_3)_{0.10}] \cdot 0.532\text{H}_2\text{O} \cdot 0.004(\text{Toluene})$	2.95	2.86	2.91	4.17	4.14	4.16
	48 h	0.630	0.001	$[\text{Mg}_{0.80}\text{Al}_{0.20}(\text{OH})_2(\text{CO}_3)_{0.10}] \cdot 0.630\text{H}_2\text{O} \cdot 0.001(\text{Toluene})$	2.56	2.62	2.59	4.27	4.33	4.30
	72 h	0.486	0.005	$[\text{Mg}_{0.80}\text{Al}_{0.20}(\text{OH})_2(\text{CO}_3)_{0.10}] \cdot 0.486\text{H}_2\text{O} \cdot 0.005(\text{Toluene})$	2.96	3.03	3.00	4.10	4.06	4.08
Hexane	4 h	0.548	0.002	$[\text{Mg}_{0.80}\text{Al}_{0.20}(\text{OH})_2(\text{CO}_3)_{0.10}] \cdot 0.548\text{H}_2\text{O} \cdot 0.002(\text{Hexane})$	2.66	2.63	2.65	4.19	4.19	4.19
	24 h	0.596	0.006	$[\text{Mg}_{0.80}\text{Al}_{0.20}(\text{OH})_2(\text{CO}_3)_{0.10}] \cdot 0.596\text{H}_2\text{O} \cdot 0.006(\text{Hexane})$	2.94	2.99	2.97	4.35	4.28	4.32
	48 h	0.518	0.003	$[\text{Mg}_{0.80}\text{Al}_{0.20}(\text{OH})_2(\text{CO}_3)_{0.10}] \cdot 0.518\text{H}_2\text{O} \cdot 0.003(\text{Hexane})$	2.80	2.71	2.76	4.13	4.18	4.16
	72 h	0.550	0.004	$[\text{Mg}_{0.80}\text{Al}_{0.20}(\text{OH})_2(\text{CO}_3)_{0.10}] \cdot 0.550\text{H}_2\text{O} \cdot 0.004(\text{Hexane})$	2.80	2.74	2.77	4.16	4.26	4.21
	96 h	0.356	0.017	$[\text{Mg}_{0.80}\text{Al}_{0.20}(\text{OH})_2(\text{CO}_3)_{0.10}] \cdot 0.356\text{H}_2\text{O} \cdot 0.017(\text{Hexane})$	4.08	4.15	4.12	4.09	4.05	4.07
	120 h	0.211	0.020	$[\text{Mg}_{0.80}\text{Al}_{0.20}(\text{OH})_2(\text{CO}_3)_{0.10}] \cdot 0.211\text{H}_2\text{O} \cdot 0.020(\text{Hexane})$	4.41	4.50	4.46	3.83	3.87	3.85

Table S3. Summary of water (*b*) and solvent (*c*) content in the AMO-LDHs and AIM-LDHs compared to conventional C-LDHs with different Mg/Al ratios LDHs as determined by elemental analysis.

Washing solvent		Formula of LDHs*	%C			%H		
			#1	#2	Average	#1	#2	Average
Mg/Al = 2	Water	$[\text{Mg}_{0.67}\text{Al}_{0.33}(\text{OH})_2(\text{CO}_3)_{0.125}] \cdot 0.415\text{H}_2\text{O}$	2.42	2.36	2.39	3.87	3.94	3.91
	Diethyl ether	$[\text{Mg}_{0.67}\text{Al}_{0.33}(\text{OH})_2(\text{CO}_3)_{0.125}] \cdot 0.246\text{H}_2\text{O} \cdot 0.044(\text{Diethyl ether})$	5.26	5.28	5.27	4.00	4.06	4.03
Mg/Al = 3	Water	$[\text{Mg}_{0.75}\text{Al}_{0.25}(\text{OH})_2(\text{CO}_3)_{0.125}] \cdot 0.461\text{H}_2\text{O}$	2.29	2.37	2.33	4.04	3.96	4.00
	Ethanol	$[\text{Mg}_{0.75}\text{Al}_{0.25}(\text{OH})_2(\text{CO}_3)_{0.125}] \cdot 0.396\text{H}_2\text{O} \cdot 0.176(\text{Ethanol})$	7.55	7.66	7.61	4.79	4.83	4.81
	Diethyl ether	$[\text{Mg}_{0.75}\text{Al}_{0.25}(\text{OH})_2(\text{CO}_3)_{0.125}] \cdot 0.182\text{H}_2\text{O} \cdot 0.086(\text{Diethyl ether})$	7.83	7.88	7.86	4.32	4.34	4.33
Mg/Al = 4	Water	$[\text{Mg}_{0.80}\text{Al}_{0.20}(\text{OH})_2(\text{CO}_3)_{0.125}] \cdot 0.634\text{H}_2\text{O}$	2.39	2.46	2.43	4.26	4.33	4.30
	Ethanol	$[\text{Mg}_{0.80}\text{Al}_{0.20}(\text{OH})_2(\text{CO}_3)_{0.125}] \cdot 0.245\text{H}_2\text{O} \cdot 0.215(\text{Ethanol})$	8.93	8.99	8.96	4.79	4.78	4.79
	Diethyl ether	$[\text{Mg}_{0.80}\text{Al}_{0.20}(\text{OH})_2(\text{CO}_3)_{0.125}] \cdot 0.370\text{H}_2\text{O} \cdot 0.021(\text{Diethyl ether})$	3.76	3.83	3.80	4.01	4.09	4.05

4. Supplementary molecular simulation data

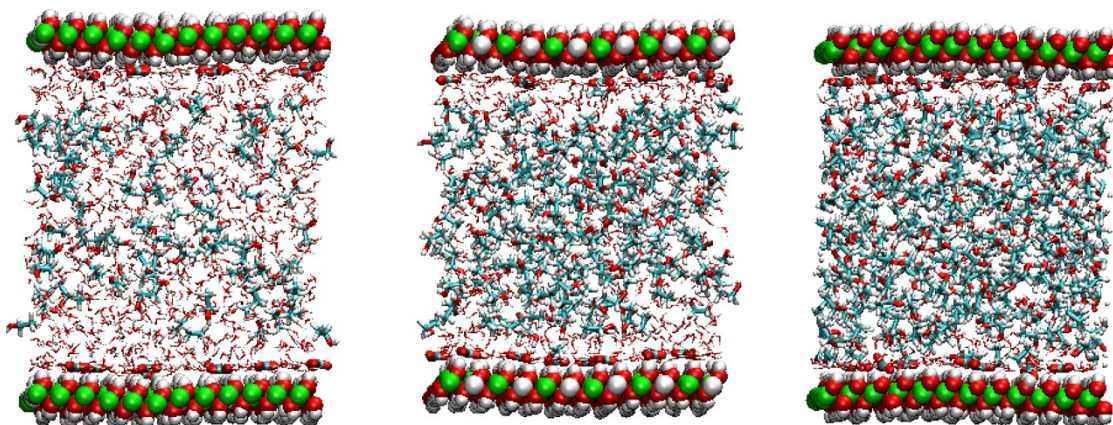


Fig. S9 Examples of simulation systems containing LDH (large spheres periodically represented on both sides of simulation box Mg - green, Al - white, O - red, H - small white) washed with ethanol (thick lines C - cyan, O - red, H - white), counterbalancing carbonate ions at the surface (thick lines C - cyan, O - red) and water shown in thin lines (O - red, H- white). From left to right concentrations are: 100 solvent - 1000 water, 200 solvent – 600 water and 300 solvent – water.

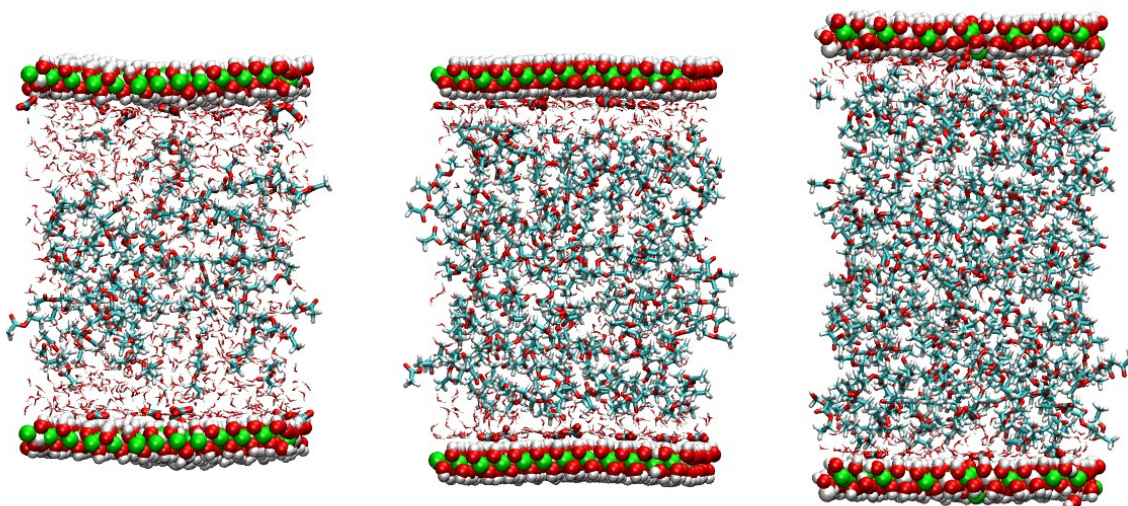


Fig. S10 Examples of simulation systems containing LDH (large spheres periodically represented on both sides of simulation box Mg - green, Al - white, O - red, H - small white) washed with ethyl acetate (thick lines C - cyan, O - red, H - white), counterbalancing carbonate ions at the surface (thick lines C - cyan, O - red) and water shown in thin lines (O - red, H- white). From left to right concentrations are: 100 solvent - 1000 water, 200 solvent - 600 water and 300 solvent - 300 water.

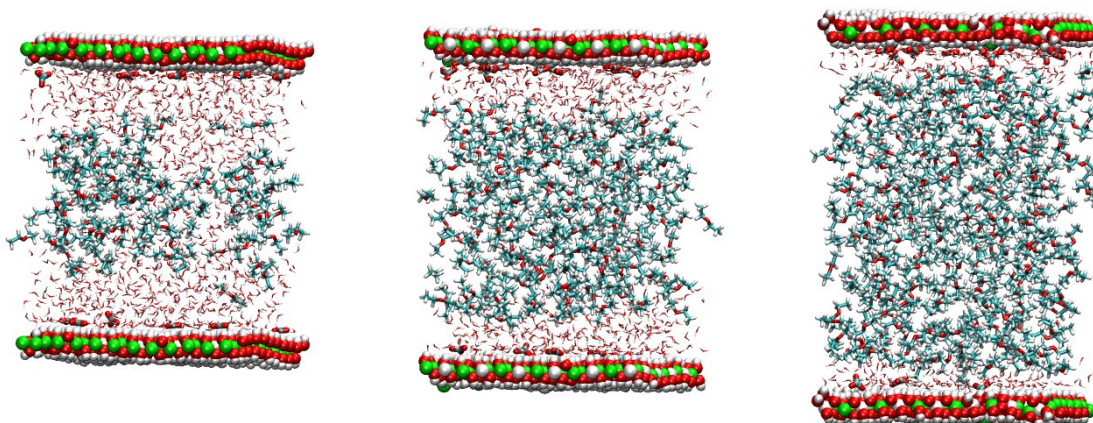


Fig. S11 Examples of simulation systems containing LDH (large spheres periodically represented on both sides of simulation box Mg - green, Al - white, O - red, H - small white) washed with diethyl ether (thick lines C - cyan, O - red, H - white), counterbalancing carbonate ions at the surface (thick lines C - cyan, O - red) and water shown in thin lines (O - red, H - white). From left to right concentrations are: 100 solvent - 1000 water, 200 solvent - 600 water and 300 solvent - 300 water.

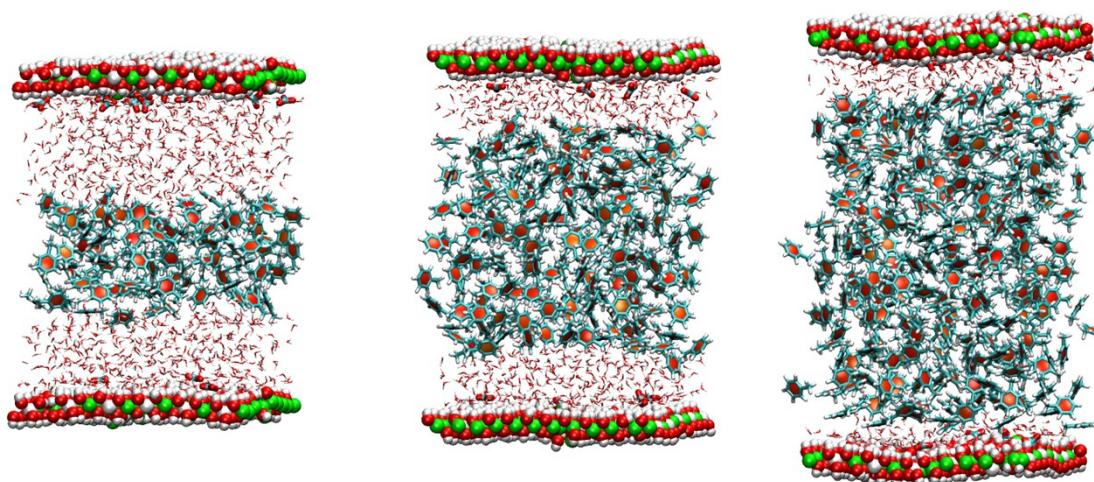


Fig. S12 Examples of simulation systems containing LDH (large spheres periodically represented on both sides of simulation box Mg - green, Al - white, O - red, H - small white) washed with toluene (thick lines C - cyan, H - white), counterbalancing carbonate ions at the surface (thick lines C - cyan, O - red) and water shown in thin lines (O - red, H - white). From left to right concentrations are: 100 solvent - 1000 water, 200 solvent - 600 water and 300 solvent - 300 water.

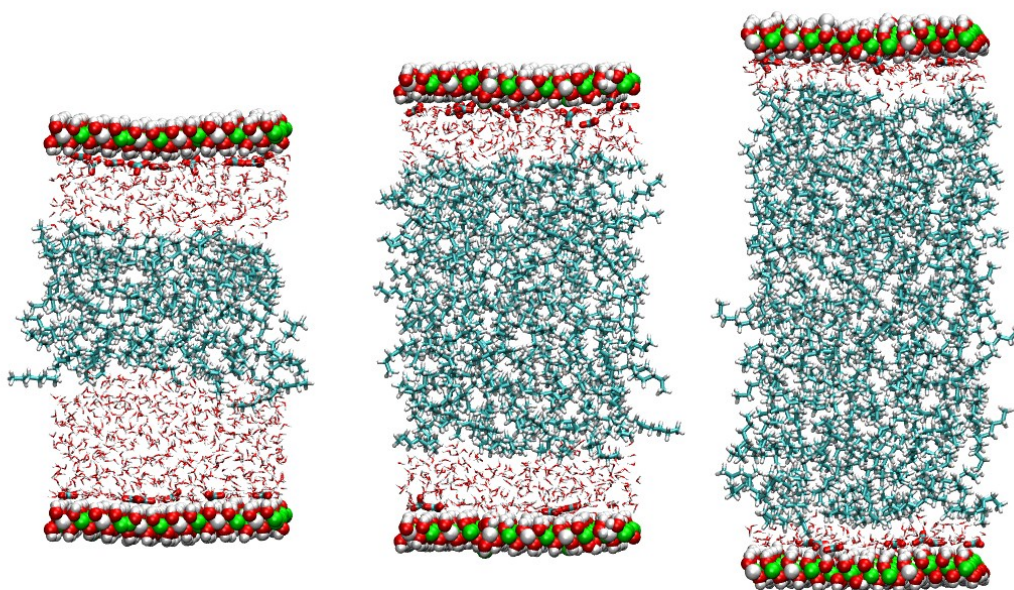


Fig. S13 Examples of simulation systems containing LDH (large spheres periodically represented on both sides of simulation box Mg - green, Al - white, O - red, H - small white) washed with hexane (thick lines C - cyan, H - white), counterbalancing carbonate ions at the surface (thick lines C - cyan, O - red) and water shown in thin lines (O - red, H- white). From left to right concentrations are: 100 solvent - 1000 water, 200 solvent - 600 water and 300 solvent - 300 water.

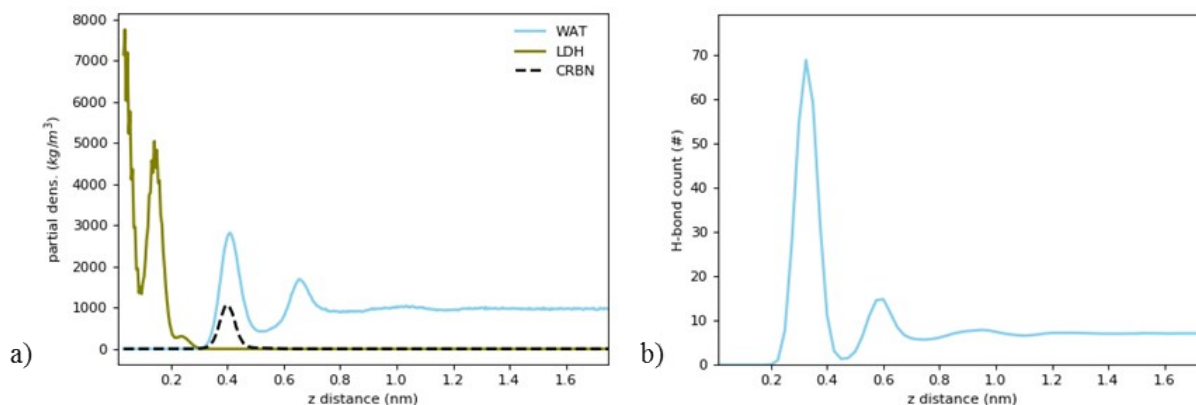


Fig. S14 a) partial densities of the LDH - water system and b) H-bonding between all system components.

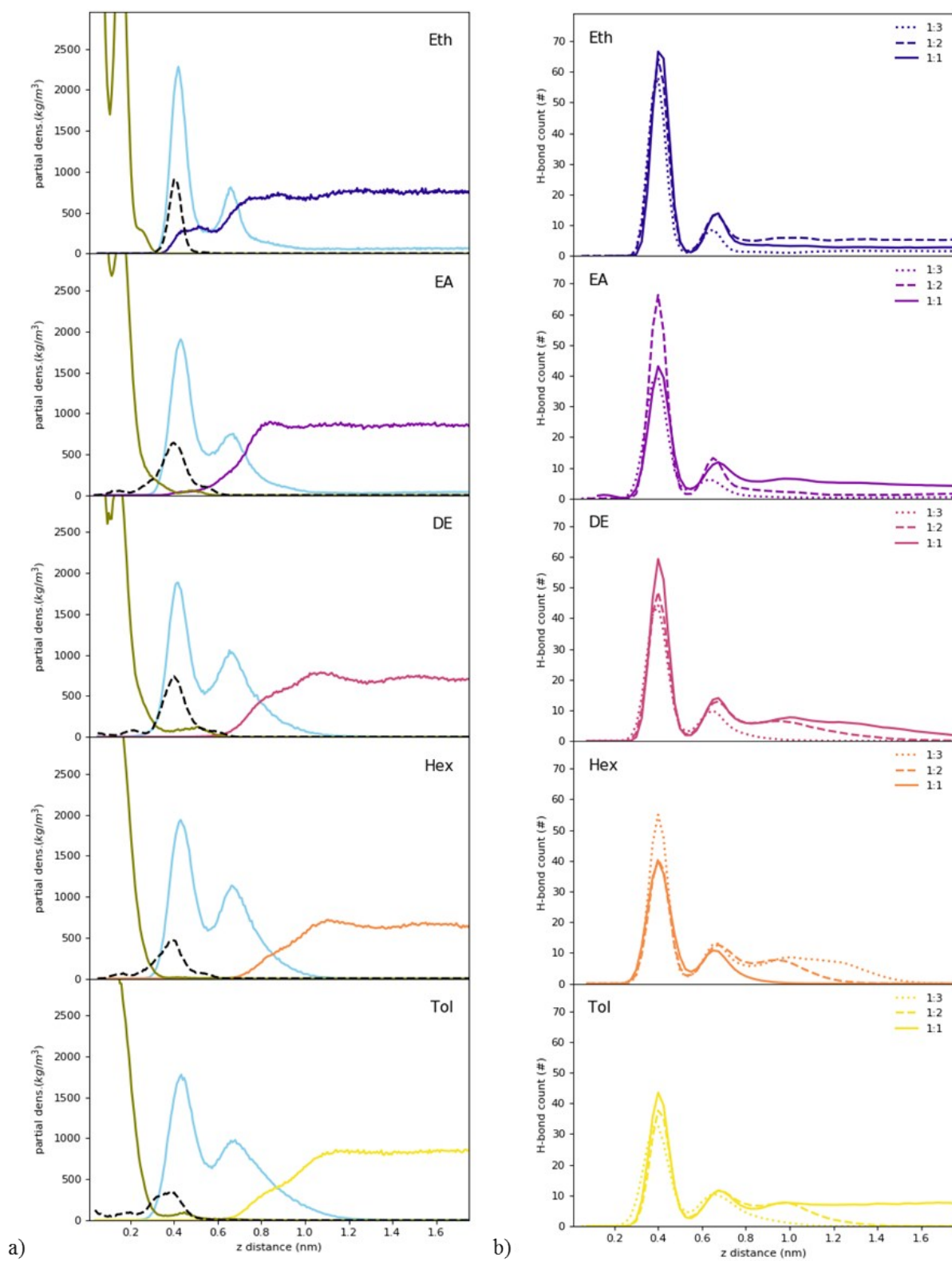


Fig. S15 a) partial densities of the LDH - 300 solvent - 300 water systems and b) H-bonding between all system components per each solvent system at three solvent - water concentrations.

5. References

1. R. T. Cygan, J.-J. Liang and A. G. Kalinichev, *J. Phys. Chem. B*, **2004**, *108*, 1255–1266
2. K. Vanommeslaeghe, E. Hatcher, C. Acharya, S. Kundu, S. Zhong, J. Shim, E. Darian, O. Guvench, P. Lopes, I. Vorobyov and A. D. Mackerell, *J. Comput. Chem.*, 2010, *31*, 671–690
3. E. Lindahl, P. Bjelkmar, P. Larsson, M. A. Cuendet and B. Hess, *J. Chem. Theory Comput.*, **2010**, *6*, 459–466
4. K. Vanommeslaeghe and A. D. MacKerell, *J. Chem. Inf. Model.*, **2012**, *52*, 3144–3154
5. I. Vorobyov, W. F. D. Bennett, D. P. Tieleman, T. W. Allen and S. Noskov, *J. Chem. Theory Comput.*, **2012**, *8*, 618–628
6. T. Underwood, V. Erastova, P. Cubillas and H. C. Greenwell, *J. Phys. Chem. C*, **2015**, *119*, 7282–7294
7. T. Underwood, V. Erastova and H. C. Greenwell, *J. Phys. Chem. C*, **2016**, *120*, 11433–11449
8. D. Van Der Spoel, E. Lindahl, B. Hess, G. Groenhof, A. E. Mark and H. J. C. Berendsen, *J. Comput. Chem.*, **2005**, *26*, 1701–1718
9. S. Pronk, S. Páll, R. Schulz, P. Larsson, P. Bjelkmar, R. Apostolov, M. R. Shirts, J. C. Smith, P. M. Kasson, D. Van Der Spoel, B. Hess and E. Lindahl, *Bioinformatics*, **2013**, *29*, 845–854